

RESEARCH

Open Access



# Long non-coding RNA MIR4435-2HG modulates pancreatic cancer stem cells and chemosensitivity to gemcitabine by targeting the miR-1252-5p/STAT1

Baocheng Xie<sup>1†</sup>, Peishan Wu<sup>4†</sup>, Hongyu Liu<sup>4</sup>, XiangDi Yang<sup>1,2,3\*</sup> and Linxuan Huang<sup>1\*</sup> 

## Abstract

Cancer stem cells (CSCs) are key drivers of cancer progression and therapeutic resistance. Long non-coding RNAs (lncRNAs) have emerged as critical regulators of CSC properties. The aim of this study was to investigate the role of MIR4435-2HG in regulating CSC characteristics, tumorigenesis, and chemoresistance in pancreatic cancer. Functional assays were conducted to evaluate CSC self-renewal, tumorigenic potential, and chemoresistance in pancreatic cancer cells with altered expression of MIR4435-2HG. RNA interference (RNAi) was employed to knock down MIR4435-2HG, and a STAT1 reintroduction model was established to examine downstream signaling pathways. The role of miR-1252-5p as a competing endogenous RNA was also explored. Overexpression of MIR4435-2HG significantly enhanced CSC self-renewal and tumorigenic potential, whereas silencing MIR4435-2HG notably diminished these properties. Mechanistically, MIR4435-2HG promoted STAT1 expression by sponging miR-1252-5p, thereby enhancing CSC stemness and tumorigenesis. Moreover, depletion of MIR4435-2HG sensitized pancreatic cancer cells to gemcitabine-induced growth inhibition and ferroptosis. Reintroduction of STAT1 restored gemcitabine resistance in MIR4435-2HG-deficient cells. Our findings demonstrate that MIR4435-2HG plays a critical role in pancreatic cancer progression by modulating CSC properties and chemoresistance through the MIR4435-2HG/miR-1252-5p/STAT1 axis. Targeting MIR4435-2HG presents a promising therapeutic approach to regulate CSCs and improve the efficacy of chemotherapy in pancreatic cancer.

**Keywords** MIR4435-2HG, Pancreatic cancer, Cancer stem cells, Ferroptosis, Chemosensitivity

<sup>†</sup>Baocheng Xie and Peishan Wu contributed equally to this work.

\*Correspondence:

XiangDi Yang

yxd323612323@126.com

Linxuan Huang

huanglx6@mail2.sysu.edu.cn

<sup>1</sup>Dongguan Key Laboratory of Precision Diagnosis and Treatment for Tumors, Dongguan Institute of Clinical Cancer Research, Department of

Pharmacy, The Tenth Affiliated Hospital of Southern Medical University (Dongguan People's Hospital), Dongguan 523059, China

<sup>2</sup>Department of Oncology, The First People's Hospital of Chenzhou, Chenzhou 423000, China

<sup>3</sup>Department of oncology, The First Affiliated Hospital of Jinan University, Guangzhou 510632, China

<sup>4</sup>Department of Pharmacology, Guangdong Medical University, Zhanjiang, Guangdong 523000, China



© The Author(s) 2025, corrected publication 2025. **Open Access** This article is licensed under a Creative Commons Attribution-NonCommercial-NoDerivatives 4.0 International License, which permits any non-commercial use, sharing, distribution and reproduction in any medium or format, as long as you give appropriate credit to the original author(s) and the source, provide a link to the Creative Commons licence, and indicate if you modified the licensed material. You do not have permission under this licence to share adapted material derived from this article or parts of it. The images or other third party material in this article are included in the article's Creative Commons licence, unless indicated otherwise in a credit line to the material. If material is not included in the article's Creative Commons licence and your intended use is not permitted by statutory regulation or exceeds the permitted use, you will need to obtain permission directly from the copyright holder. To view a copy of this licence, visit <http://creativecommons.org/licenses/by-nc-nd/4.0/>.

## Introduction

The five-year survival rate for pancreatic cancer (PC) is less than 10%, making it one of the most aggressive gastrointestinal cancers. Typically, the disease remains asymptomatic until it has reached an advanced stage, which contributes to its poor prognosis. High mortality in pancreatic cancer primarily stems from its resistance to current therapies and the frequent occurrence of metastasis at the time of diagnosis [1]. Therefore, elucidating the mechanisms underlying PC progression is essential for developing more effective therapeutic and early diagnostic approaches.

Cancer stem cells (CSCs), also known as tumor-initiating cells, possess remarkable abilities of self-renewal and proliferation [2]. CSCs possess stem-like characteristics that enable them to sustain tumor growth and contribute to long-term tumor maintenance [3]. There is extensive evidence that CSCs play a key role in cancer biology, such as tumor initiation, recurrence, and resistance to chemotherapy. However, the exact mechanisms underlying the spread of pancreatic cancer CSCs remain largely elusive.

Long non-coding RNAs (lncRNAs) are RNA molecules longer than 200 nucleotides that cannot encode proteins [4, 5]. The lncRNA regulator of reprogramming is highly expressed in both embryonic stem cells and induced pluripotent stem cells [6]. It has been identified as an essential factor in pluripotent transcription factors like Sox2, Oct4, and Nanog reprogramming differentiated cells into iPSCs [7]. MIR4435-2HG has been implicated in multiple malignancies as a carcinogenic lncRNA. Its abnormal expression is closely associated with critical processes in cancer biology [8, 9]. In addition, elevated levels of MIR4435-2HG are associated with various clinicopathological characteristics, including tumor size, TNM stage, and lymph node metastasis [10]. By acting as a competing endogenous RNA, MIR4435-2HG promotes cancer progression by sponging of specific miRNAs, thereby regulating cancer initiation, metastasis and epithelial-to-mesenchymal transition. However, its exact role in pancreatic cancer stem cell remains to be fully elucidated.

The aim of our study was to investigate the role of MIR4435-2HG in pancreatic cancer cells and to identify its underlying mechanisms. Our findings demonstrate that MIR4435-2HG not only modulates the expression of miR-1252-5p but also affects the activity of the STAT1 signaling pathway. Additionally, we found that dysregulation of MIR4435-2HG plays a role in pancreatic cancer stem cells and chemoresistance by inhibiting ferroptosis. Overall, our study underscores the significance of long non-coding RNAs in cancer biology and highlights the potential of the MIR4435-2HG/miR-1252-5p/STAT1 axis as a novel therapeutic target for pancreatic cancer.

## Materials and methods

### Ethics statement

Our study was approved by the Tenth Affiliated Hospital of Southern Medical University (Dongguan People's Hospital), and all animal experiments were performed following the guidelines outlined in the Guide for the Care and Use of Laboratory Animals.

### Gene expression profiling

We investigated the expression of MIR4435-2HG and STAT1, along with their prognostic implications for pancreatic cancer patients in The Cancer Genome Atlas (TCGA) (<http://bioinfo.life.hust.edu.cn/GSCA/#/>). Potential target miRNAs for MIR4435-2HG were predicted through the starBase 3.0 database (<http://starbase.sysu.edu.cn/>).

### Cell culture

We obtained normal pancreatic ductal epithelial cells (HPNE) and pancreatic ductal adenocarcinoma cell lines (BxPC-3 and PANC-1) from the Shanghai Institute of Cell Biology, Chinese Academy of Sciences (Shanghai, China). Cells were cultured in DMEM (Gibco, USA) with 10% FBS, 100 U/mL penicillin, and 0.1 mg/mL streptomycin.

### Cell transfection

The MIR4435-2HG or STAT1 overexpression plasmids, as well as scramble siRNA (NCsi) and siRNAs targeting MIR4435-2HG (siMIR4435-2HG), were purchased from Igebio (China). For transfection, the target plasmid and Lipofectamine 3000 (Invitrogen, USA) were diluted separately in 250  $\mu$ L of Opti-MEM (Gibco, USA) and incubated for 5 min. The two solutions were incubated for an additional 20 min. After 48 h, the cells were treated with 5  $\mu$ g/mL puromycin.

### qRT-PCR and western blotting analysis

Reagents used for qRT-PCR were purchased from Vazyme (China). The Primer sequences used for performing qRT-PCR assay are shown as Table 1. The primary and second antibodies used for western blotting of CD44, KLF4, OCT4, SOX2, GPX4, SLC7A11, Ki67, STAT1 and GAPDH were all purchased from Proteintech (China), the dilution ratio is according to the instructions.

### CCK8 assay

Transfected BxPC-3 and PANC-1 cells ( $5 \times 10^3$  cells/well) were seeded into a 96-well plate. Subsequently, 10  $\mu$ L of CCK8 solution was added. After 2 h incubation, the absorbance at 450 nm was measured using a microplate reader (Thermo, USA).

**Table 1** Primer sequence

Gene	Primer sequence
MIR4435-2HG-F	5'- CGGAGCATGGAACCTCGACAG -3'
MIR4435-2HG-R	5'- CAAGTCTCACACATCCGGGG -3'
CD44-F	5'- CACACCCTCCCCTCATTAC -3'
CD44-R	5'- CAGCTGTCCCTGTTGTGCAG -3'
KLF4-F	5'- GTCCCGGGGATTGTAGCTC -3'
KLF4-R	5'- CGTCTCCCTCTTTGGCTT -3'
OCT4-F	5'- AAACCCACACTGCAGCAGATCA -3'
OCT4-R	5'- CCCCTGAGAAAGGAGACCCA -3'
SOX2-F	5'- CATGAAGGAGACCCGGATT -3'
SOX2-R	5'- TTCATGTGCGCGTAACTGTC -3'
miR-1252-5p-RT	5'- gAAAgAAggCgAggAgCAGATC- gAggAAgAAgACggAAgAATgTgC- gTCTCgCCTTCTTTCTAAATgAA -3'
miR-1252-5p-F	5'- ggTggAgggAgAAggAAATgAA -3'
U6-F	5'- CTCgCTTCggCAGCAC -3'
U6-R	5'- AACgCTTCACgAATTgCgT -3'
STAT1-F	5'- TCTGGAAAACGCCAGAGATT -3'
STAT1-R	5'- CTACTTCTCTGTTCTGCAAGG -3'
GAPHD-F	5'- CAAATTCCATGGCACCGTCA -3'
GAPHD-R	5'- TGATGACCCCTTTGGCTCCC -3'

#### Cell sphere formation assay

A total of  $7 \times 10^5$  BxPC-3 or PANC-1 cells were seeded into a 10 cm<sup>2</sup> ultralow-adhesion culture flask containing DMEM supplemented with 10 ng/mL bFGF, 20 ng/mL EGF, 5 µg/mL insulin, B27, 100 units/mL penicillin, and 100 µg/mL streptomycin. The cell spheres were counted in each visual field, with cell clusters measuring  $\geq 50$  µm in diameter considered as successfully formed spheres.

#### Colony formation assay

Cells were plated in six-well plates at a density of 800 cells and incubated at 37 °C with 5% CO<sub>2</sub> for 15 days. Following incubation, the medium was removed, and the cells were fixed with 4% paraformaldehyde for 15 min. Subsequently, the cells were stained with crystal violet for 30 min. Clones were imaged and counted.

#### Immunohistochemistry

The tissues were fixed in 4% paraformaldehyde, embedded in paraffin, and sectioned. Tissue sections were incubated with 100 µL of primary antibody at room temperature for 1 h. Then, 50 µL of goat anti-rabbit IgG secondary antibody (SA00001, 1:5000, Proteintech, China) was applied and incubated at room temperature for 1 h. Next, the sections were treated with streptavidin peroxidase at 37 °C for 30 min. Afterward, they were incubated with diaminobenzidine for 10 min and counterstained with hematoxylin for 2 min. The sections were differentiated using hydrochloric ethanol, rinsed in water for 10 min, and finally observed under a microscope.

#### RNA-pull down assay

Cells were transfected with 50 nM biotin-labeled miR-1252-5p-WT and miR-1252-5p-MUT. Cell lysates were prepared using polysome buffer containing a protease inhibitor cocktail and RNase inhibitor. Separately, cell lysates and biotin-labeled RNA were each incubated with Streptavidin Dynabeads (Invitrogen) for 1 h. Following this, cell lysates were added to the RNA-bound beads, and the mixtures were rotated at 4 °C for 2–4 h. The beads were then washed three times with NT2 buffer, twice with high-salt NT2 buffer (NT2 with 500 mM NaCl), and once with PBS, each wash lasting 5 min at 4 °C. Finally, 50 µL of 2× SDS loading buffer was added, and the samples were heated at 100 °C for 10 min. The enrichment of MIR4435-2HG was subsequently analyzed by RT-qPCR.

#### RNA immunoprecipitation (RIP) assay

The RIP assay was conducted using the Magna RIP RNA Binding Protein Immunoprecipitation Kit (Bersinbio, China). Cell lysates were prepared and incubated in RIP buffer with magnetic beads conjugated to either a human anti-Agonate2 (anti-Ago2) antibody (Proteintech) or IgG control. RNA was then extracted from the immunoprecipitates and analyzed by qRT-PCR.

#### Dual-luciferase reporter gene assay

Cells were plated in 6-well plates at a density of  $5 \times 10^5$ . Designated wells were co-transfected with the respective vector and miR-1252-5p mimics. According to the manufacturer's instructions (Ribobio, Guangzhou), cell lysates were collected to measure both firefly and Renilla luciferase activities. The relative luciferase activity was then normalized to the firefly luciferase control.

#### Tumor xenograft in nude mice

MIR4435-2HG knockdown BxPC-3 cells were subcutaneously injected into BALB/c nude mice (female, 4 weeks old). The mice were weighted weekly and euthanized 7 weeks after injection.

#### Measurement of ATP level

Cells were plated in 6-well plates at a density of  $5 \times 10^5$  cells and incubated for 24 h. After a subsequent treatment period of 48 h, the cells were collected and lysed. ATP levels were assessed by combining 20 µL of the cell supernatant with 100 µL of luciferase reagent, following the protocol provided in the ATP Assay Kit (Beyotime, China).

#### Reactive oxygen species fluorometric assay

We employed the Reactive Oxygen Species Fluorometric Assay Kit (E-BC-F005, Elabscience) to evaluate ROS accumulation. In brief, cells were rinsed twice with cold

PBS. A 50  $\mu$ M working solution was then added to the samples, which were incubated for 1 h at 37 °C. Finally, the samples were analyzed by flow cytometry.

#### Intracellular iron assessment

We used the Cell Ferrous Iron Fluorometric Assay Kit (E-BC-F101, Elabscience) to assess changes in Fe<sup>2+</sup> concentrations. Briefly, cells were washed twice with PBS. Then, 1 mL of the Ferro working solution was added to the samples and incubated for 60 min at 37 °C. Finally, the samples were fixed for immunofluorescence staining.

#### Statistical analysis

All data are expressed as means  $\pm$  SD from a minimum of three independent experiments. Comparisons between groups were conducted using ANOVA or Student's t-test via GraphPad Prism 7 software. Kaplan-Meier curves were evaluated using log-rank tests.  $p < 0.05$  was deemed statistically significant.

## Results

### MIR4435-2HG is overexpressed in pancreatic cancer and is associated with poor prognosis

To assess the potential clinical relevance of lncRNA MIR4435-2HG expression in cancer, we first analyzed the pan-cancer gene expression using the TCGA database. MIR4435-2HG was significantly upregulated in various cancer types compared to adjacent normal tissues (Fig. 1A). Previous transcriptome sequencing studies have also shown that MIR4435-2HG is overexpressed in tumor tissues [11]. Further analysis of the TCGA database confirmed that MIR4435-2HG levels are elevated in pancreatic cancer tissues compared to adjacent normal tissues (Fig. 1B).

The relationship between MIR4435-2HG expression and the clinicopathological characteristics of pancreatic cancer patients was further examined. We found that elevated levels of MIR4435-2HG were positively correlated with higher TNM stage, lymph node metastasis, distant metastasis, and pathological grade. Additionally, within the pancreatic cancer cohort, MIR4435-2HG expression significantly increased with histologic grade, particularly in poorly differentiated (PD) and G2 tumors (Fig. 1C). Kaplan-Meier analysis indicated that pancreatic cancer patients with high MIR4435-2HG expression had poorer overall survival, disease-free survival, and progression-free intervals (Fig. 1D). Univariate Cox regression analyses were performed to assess the prognostic significance of MIR4435-2HG in these patients (Fig. 1E), revealing a significant correlation between MIR4435-2HG risk scores and overall survival (OS), thus establishing it as an independent prognostic marker. Notably, the area under the curve (AUC) of the ROC curves for predicting progression-free survival (PFS) was 0.979 (Fig. 1F),

highlighting the predictive capability of MIR4435-2HG in pancreatic cancer progression.

Additionally, we evaluated the expression of MIR4435-2HG in pancreatic cancer cell lines, finding that it was highly expressed in BxPC-3, PANC-1, and AsPC-1 cells compared to normal pancreatic ductal cells (HPNE) (Fig. 1G). Furthermore, RNA fluorescence in situ hybridization (FISH) revealed that MIR4435-2HG was primarily localized in the nucleus and cytoplasm of pancreatic cancer (Fig. 1H, Supplementary Figs. 1 and 2). Together, these findings indicate that MIR4435-2HG plays a crucial role as an oncogene in pancreatic cancer.

### MIR4435-2HG enhances the self-renewal capacity of pancreatic cancer stem cells

We conducted gene set enrichment analysis (GSEA) to explore the functional roles mediated by MIR4435-2HG. The results revealed that the most relevant biological processes included stem cell differentiation, proliferation, and development (Fig. 2A). Given the elevated expression of MIR4435-2HG in pancreatic cancer and its strong association with stem cell characteristics, we first assessed spheroid formation in ultra-low attachment plates. In our loss-of-function studies, we utilized siRNA targeting MIR4435-2HG in BxPC-3 and PANC-1 cells. The qRT-PCR results confirmed successful modulation of MIR4435-2HG expression in these cells (Fig. 2B). Spheroid formation assays demonstrated that knockdown of MIR4435-2HG significantly impaired spheroid formation capability (Fig. 2C), while overexpression of MIR4435-2HG markedly enhanced cell sphere formation in both BxPC-3 and PANC-1 cells (Fig. 3A and B). These findings indicate that MIR4435-2HG plays a crucial role in regulating pancreatic cancer stem cells (CSCs), as evidenced by a decrease in the expression of well-established CSC marker genes, including CD44, KLF4, OCT4, and Sox2 (Fig. 2D and E). In contrast, overexpression of MIR4435-2HG resulted in a significant increase in CSC markers (Fig. 3 C-3D). Additionally, the ability to form colonies was significantly reduced in MIR4435-2HG knockdown cells compared to control shRNA cells (Fig. 2F), whereas overexpression of MIR4435-2HG greatly promoted colony formation (Fig. 3E). These results suggest that MIR4435-2HG is involved in the proliferation of cancer stem cells.

### MIR4435-2HG promotes the self-renewal and tumorigenic properties of pancreatic adenocarcinoma cells by targeting miR-1252-5p

To explore the molecular mechanism by which MIR4435-2HG promotes pancreatic cancer progression, we used StarBase to predict potential microRNAs that may directly interact with MIR4435-2HG. miR-1252-5p emerged as a candidate. To confirm that MIR4435-2HG

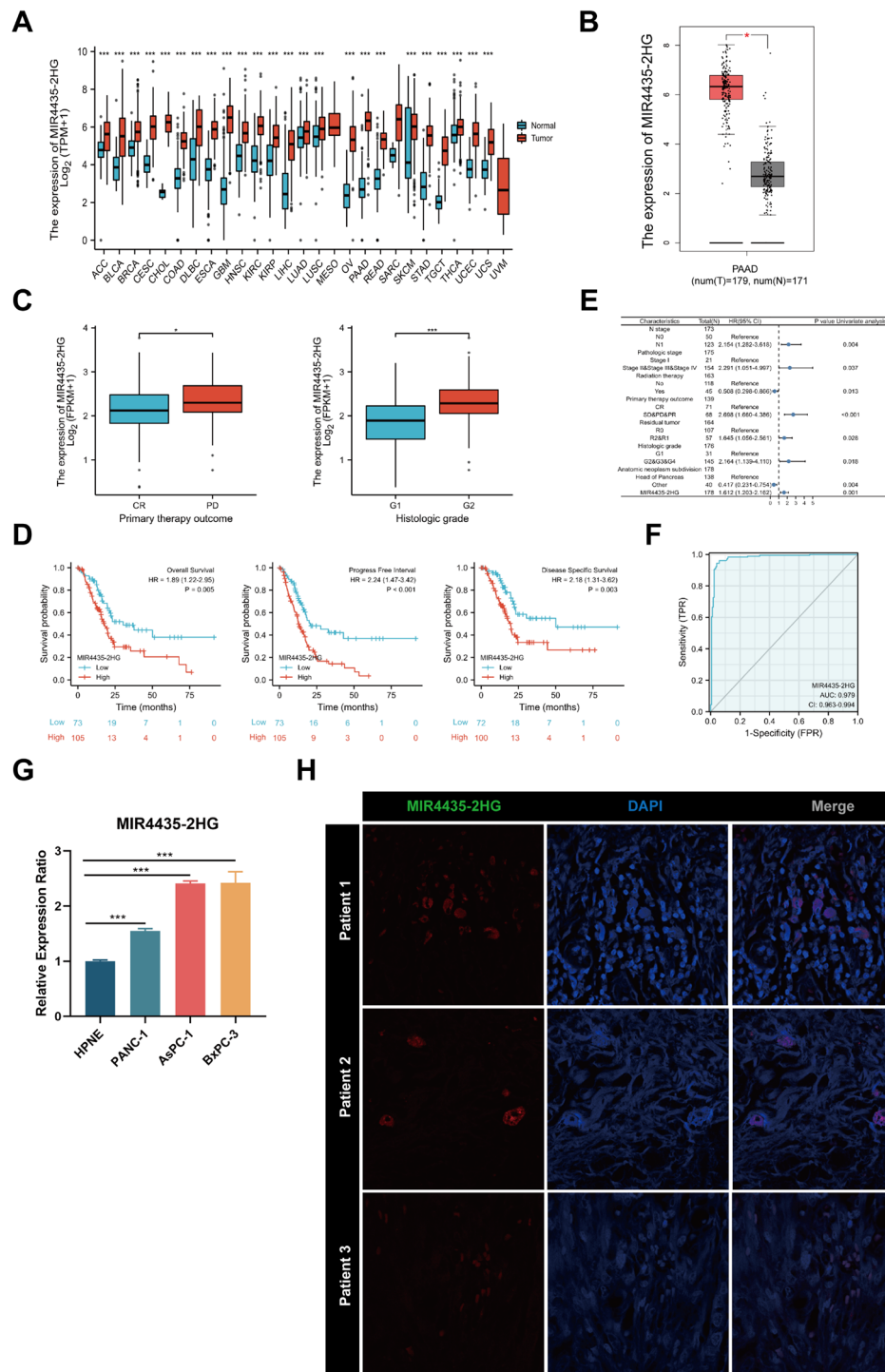


**Fig. 1** MIR4435-2HG is upregulated in pancreatic cancer and correlates with a poor prognosis **(A)** Pan-cancer analysis of MIR4435-2HG expression across the TCGA dataset. **(B)** Comparison of MIR4435-2HG expression between pancreatic cancer tissues (n=179) and normal tissues (n=171). **(C)** Correlation between MIR4435-2HG expression and clinical features, including primary therapy outcomes and histologic grade. **(D)** Kaplan-Meier survival analyses for overall survival, disease-free survival, and progression-free interval in relation to MIR4435-2HG expression levels. **(E)** Univariate Cox regression analysis of MIR4435-2HG expression in pancreatic cancer patients. **(F)** Receiver Operating Characteristic (ROC) curve for MIR4435-2HG in pancreatic cancer patients, with Area Under the Curve (AUC) = 0.979. **(G)** Quantitative PCR analysis of MIR4435-2HG expression levels in HPNE, PANC-1, AsPC-1, and BxPC-3 cell lines. **(H)** RNA fluorescence in situ hybridization (FISH) analysis was performed using a specific probe for MIR4435-2HG in pancreatic cancer samples from different patients. \*p<0.05, \*\*p<0.01, \*\*\*p<0.001

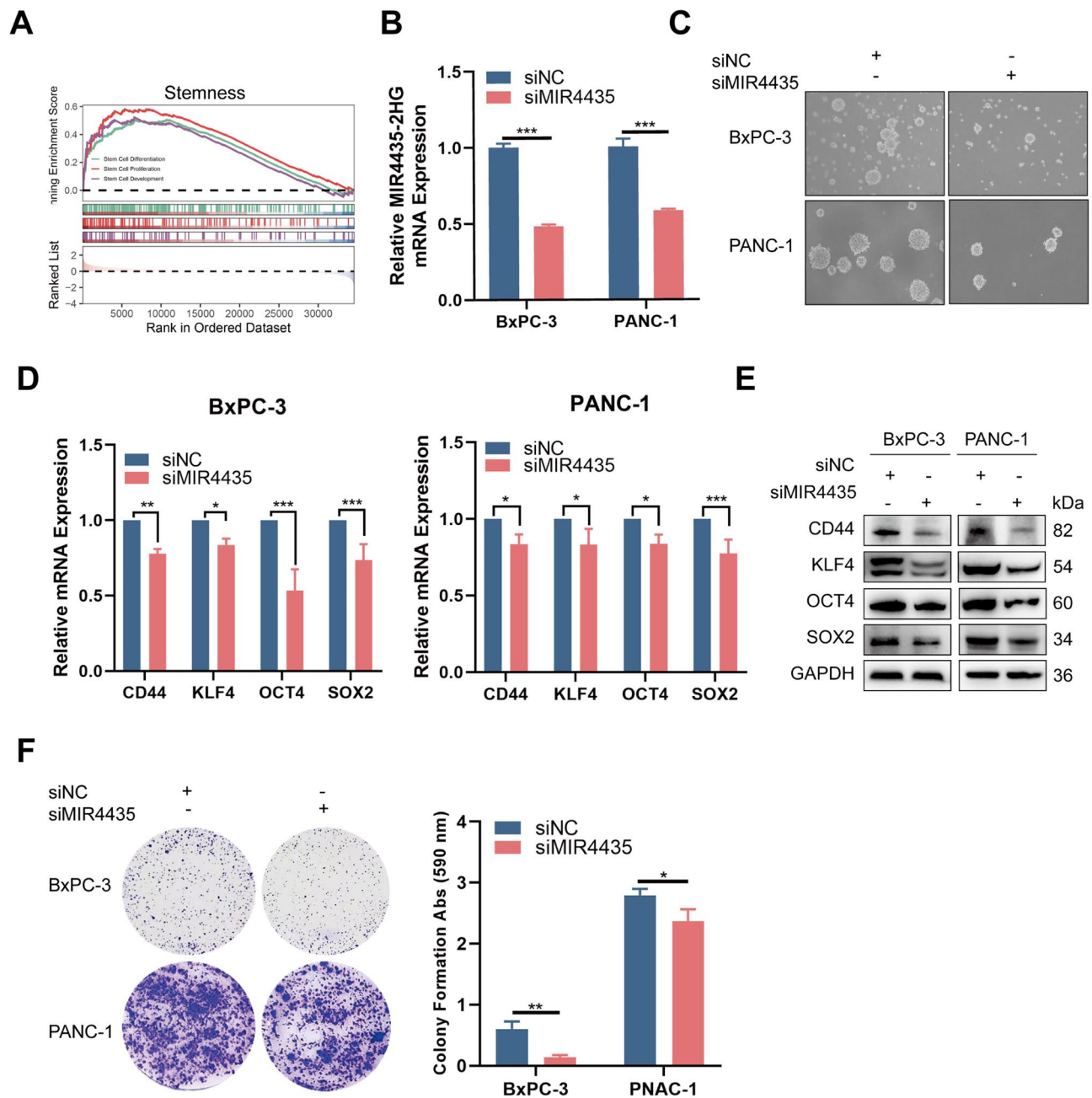


**Fig. 2** Knockdown of MIR4435-2HG suppresses pancreatic cancer stemness. **(A)** Gene Set Enrichment Analysis (GSEA) showing enrichment of MIR4435-2HG in stem cell differentiation, proliferation, and development signaling pathways. **(B)** RT-qPCR analysis of MIR4435-2HG expression in BxPC-3 and PANC-1 cells following transfection with negative control siRNA or MIR4435-2HG siRNA. **(C)** Representative images of cancer stem cell (CSC) spheres in control and siMIR4435-2HG-transfected cells. **(D)** RT-qPCR and **(E)** Western blot analysis of CD44, KLF4, OCT4, and SOX2 expression in control and siMIR4435-2HG-transfected cells. **(F)** Colony formation assay and quantification of colony numbers in BxPC-3 and PANC-1 cells with MIR4435-2HG knockdown. \* $p < 0.05$ , \*\* $p < 0.01$ , \*\*\* $p < 0.001$

specifically targets miR-1252-5p, we examined the expression levels of the candidate microRNAs and their correlation with MIR4435-2HG in pancreatic adenocarcinoma (PAAD). We constructed dual-luciferase reporters featuring either a wild-type (MIR4435-2HG-WT) or mutated (MIR4435-2HG-Mut) binding site. The luciferase activity assay demonstrated that co-transfection with

a miR-1252-5p mimic significantly reduced the relative luciferase activity of MIR4435-2HG-WT but did not affect the mutant plasmid, confirming that miR-1252-5p is a direct target of MIR4435-2HG (Fig. 4A).

Subsequently, we performed RNA pull-down assay to determine whether MIR4435-2HG directly interacts with miR-1252-5p. qRT-PCR analysis of the RNA pellet

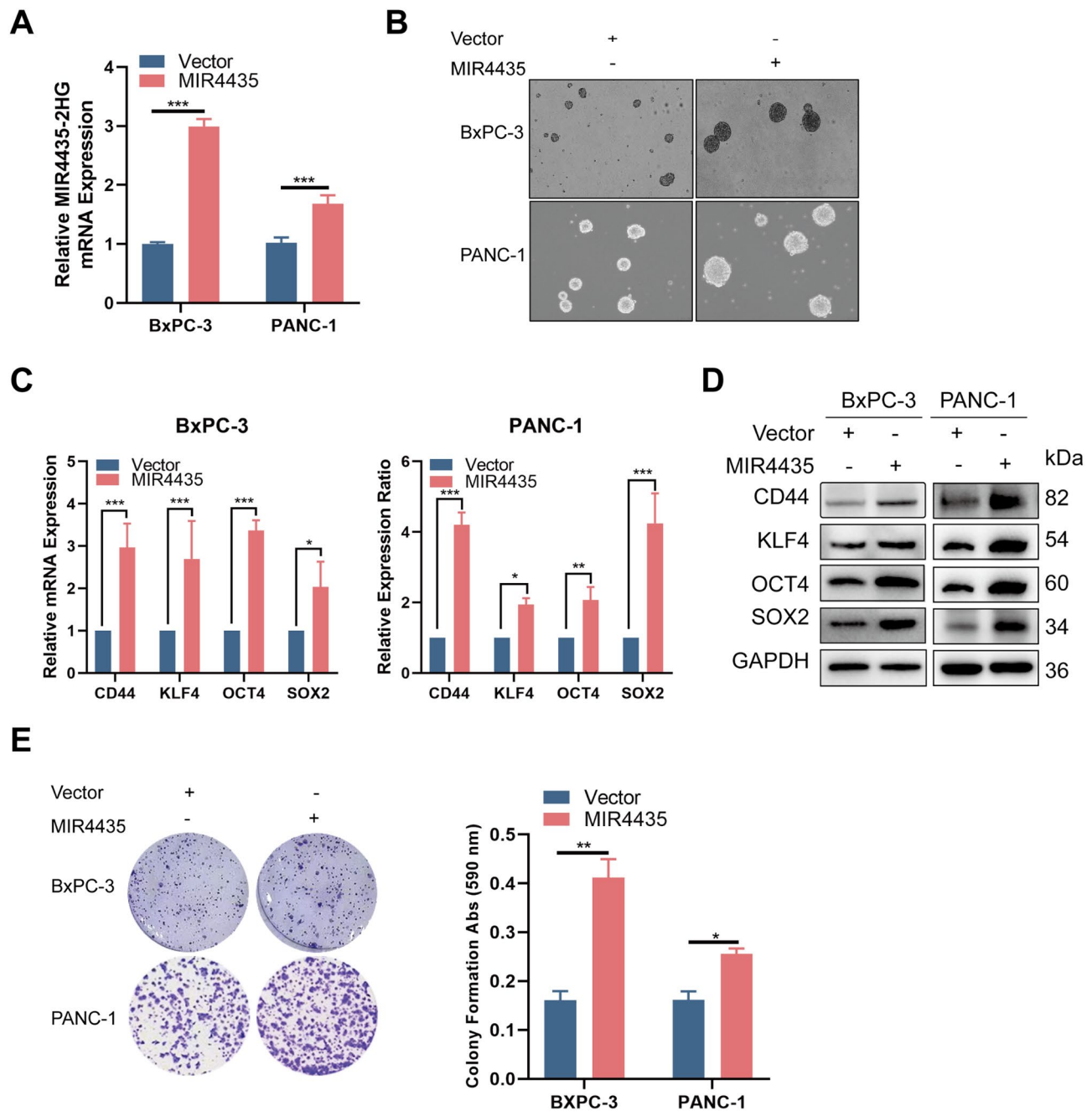


**Fig. 3** Overexpression of MIR4435-2HG enhances pancreatic cancer stemness. **(A)** RT-qPCR analysis of MIR4435-2HG expression in BxPC-3 and PANC-1 cells following transfection with either an empty vector (control) or MIR4435-2HG-overexpression vector. **(B)** Representative images of cancer stem cell (CSC) spheres in control and MIR4435-2HG-overexpressing cells. **(C)** RT-qPCR and **(D)** Western blot analyses of CD44, KLF4, OCT4, and SOX2 expression in control and MIR4435-2HG-overexpressing cells. **(E)** Colony formation assay and quantification of colony numbers in BxPC-3 and PANC-1 cells with MIR4435-2HG overexpression. \* $p < 0.05$ , \*\* $p < 0.01$ , \*\*\* $p < 0.001$

obtained from the MIR4435-2HG pull-down revealed a significant presence of miR-1252-5p (Fig. 4B). Additionally, a RIP assay utilizing a biotinylated MIR4435-2HG probe demonstrated that MIR4435-2HG binds to the AGO2 protein, with miR-1252-5p significantly enriched in the RNAs pulled down from the MIR4435-2HG complex (Fig. 4C). qRT-PCR results indicated

that miR-1252-5p expression was lower in BxPC-3 and PANC-1 cells compared to HPNE cells (Fig. 4D). Collectively, these findings suggest that MIR4435-2HG directly binds to miR-1252-5p and acts as a competitive inhibitor.

Further RT-qPCR analysis revealed that the expression of miR-1252-5p was decreased in pancreatic cancer cells upon overexpression of MIR4435-2HG and was

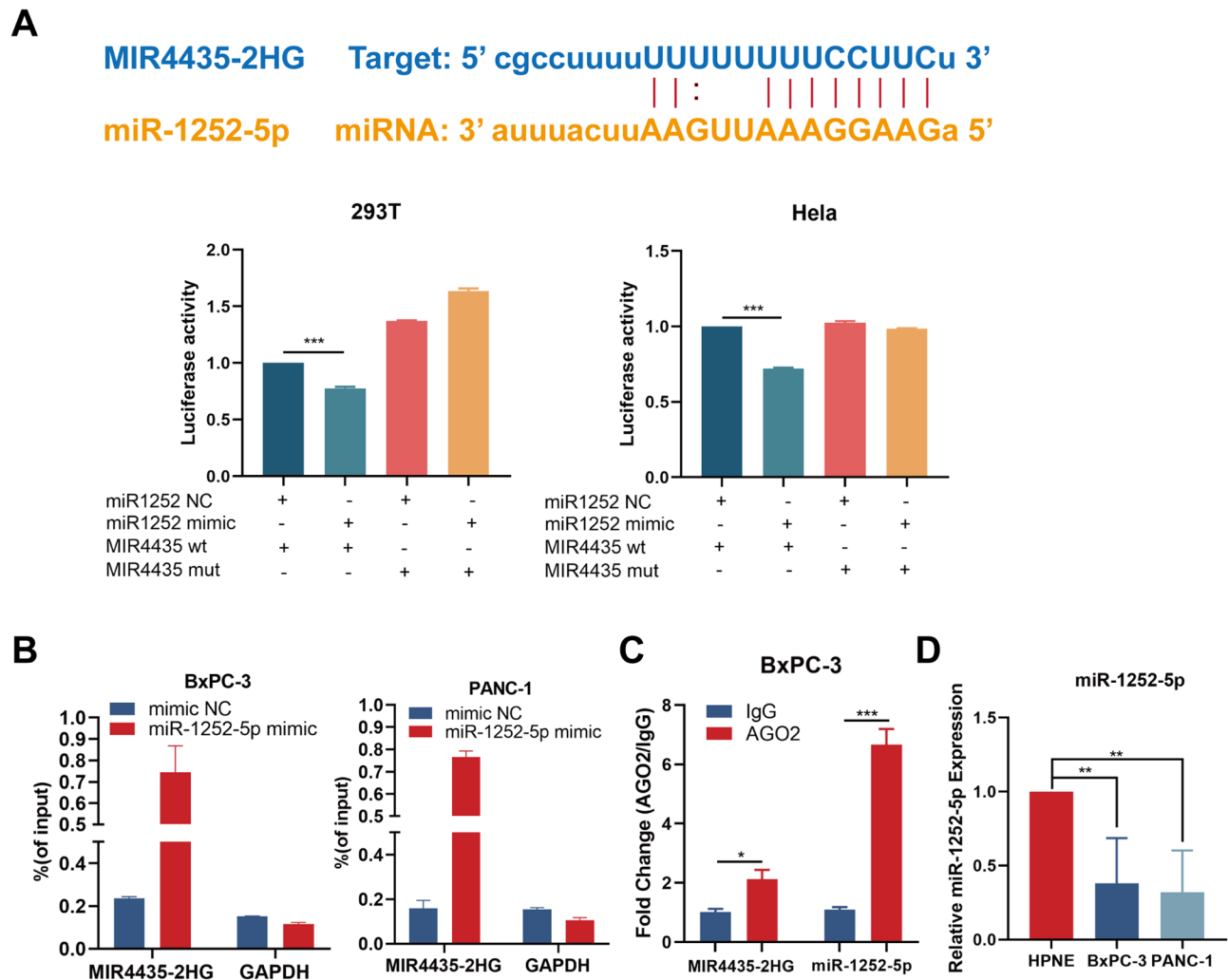


**Fig. 4** MIR4435-2HG targets miR-1252-5p in pancreatic cancer cells. (A) Predicted binding sites of MIR4435-2HG on the 3'-UTR of miR-1252-5p, along with results from the dual-luciferase reporter assay, showing a significant reduction in luciferase activity in cells transfected with wild-type miR-1252-5p luciferase vectors. (B) RNA pull-down assay demonstrating the interaction between MIR4435-2HG and miR-1252-5p in BxPC-3 and PANC-1 cells. (C) RIP assay showing the binding efficiency of MIR4435-2HG and miR-1252-5p to AGO2 protein. (D) RT-qPCR analysis of miR-1252-5p expression levels in HPNE, BxPC-3, and PANC-1 cells. \* $p < 0.05$ , \*\* $p < 0.01$ , \*\*\* $p < 0.001$

upregulated following the knockdown of MIR4435-2HG (Fig. 5A). To investigate the role of miR-1252-5p in pancreatic cancer, we transfected BxPC-3 and PANC-1 cells with either a miR-1252-5p inhibitor or mimic (Fig. 5B). Treatment with the miR-1252-5p mimic inhibited sphere formation, whereas the miR-1252-5p inhibitor enhanced it (Fig. 5C). qRT-PCR and western blot analyses demonstrated that inhibition of miR-1252-5p led to the upregulation of cancer stem cell markers, while overexpression of miR-1252-5p resulted in their downregulation (Fig. 5D and E). Moreover, the colony formation ability was decreased with miR-1252-5p mimic treatment and increased with miR-1252-5p inhibition (Fig. 5F). These results indicate that miR-1252-5p is a direct target of MIR4435-2HG, which negatively regulates miR-1252-5p expression.

#### STAT1 is a direct target of miR-1252-5p

To further predict the targets of miR-1252-5p, we used starBase and identified a binding site for miR-1252-5p in the 3' UTR of STAT1 (Fig. 6A). Transfection with miR-1252-5p mimics resulted in a significant decrease in luciferase activity for the wild-type STAT1 3' UTR (STAT1 3'UTR-WT), while no notable changes were observed in the luciferase activity of the mutated STAT1 3' UTR (STAT1 3'UTR-Mut) (Fig. 6B). We also explored the relationship between MIR4435-2HG and STAT1 using the GEPIA database, which indicated a positive correlation (Fig. 6C). Moreover, qRT-PCR assays revealed that STAT1 mRNA levels were higher in BxPC-3 and PANC-1 cells compared to HPNE cells (Fig. 6D). These results are consistent with earlier studies showing that STAT1 is overexpressed in pancreatic cancer (Fig. 6E).

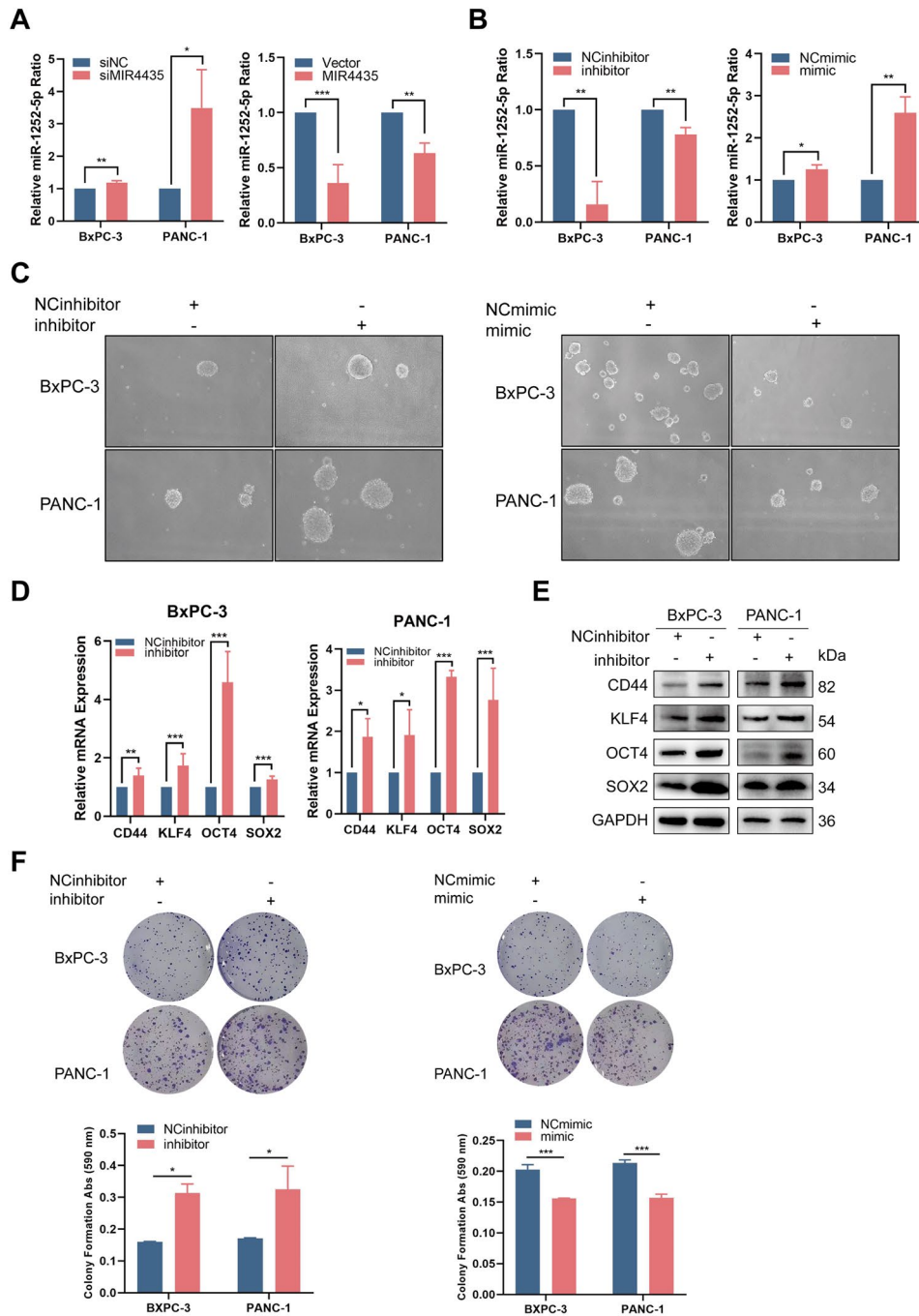


**Fig. 5** MIR4435-2HG targets miR-1252-5p to promote pancreatic cancer stemness. **(A)** RT-qPCR analysis of miR-1252-5p expression in cells with MIR4435-2HG knockdown and overexpression. **(B)** RT-qPCR analysis of miR-1252-5p expression in BxPC-3 and PANC-1 cells transfected with miR-1252-5p inhibitor or mimic. **(C)** Representative images of cancer stem cell (CSC) spheres in cells transfected with miR-1252-5p mimic or inhibitor. **(D)** RT-qPCR and **(E)** Western blot analyses of CD44, KLF4, OCT4, and SOX2 expression in cells with miR-1252-5p inhibition. **(F)** Colony formation assay and quantification of colony numbers in BxPC-3 and PANC-1 cells transfected with miR-1252-5p mimic or inhibitor. \* $p < 0.05$ , \*\* $p < 0.01$ , \*\*\* $p < 0.001$

The potential of STAT1 as a diagnostic marker in pancreatic cancers was assessed using a receiver operating characteristic (ROC) curve, resulting in an area under the curve (AUC) value of 0.961, suggesting that STAT1 could act as an independent prognostic biomarker in pancreatic cancer (Fig. 6F).

Additionally, we evaluated the correlation between STAT1 expression and clinicopathological features in the TCGA dataset. Our analysis demonstrated a positive association between STAT1 expression and tumor stage (Fig. 6G). In alignment with the TCGA cohort findings, elevated levels of STAT1 expression were significantly

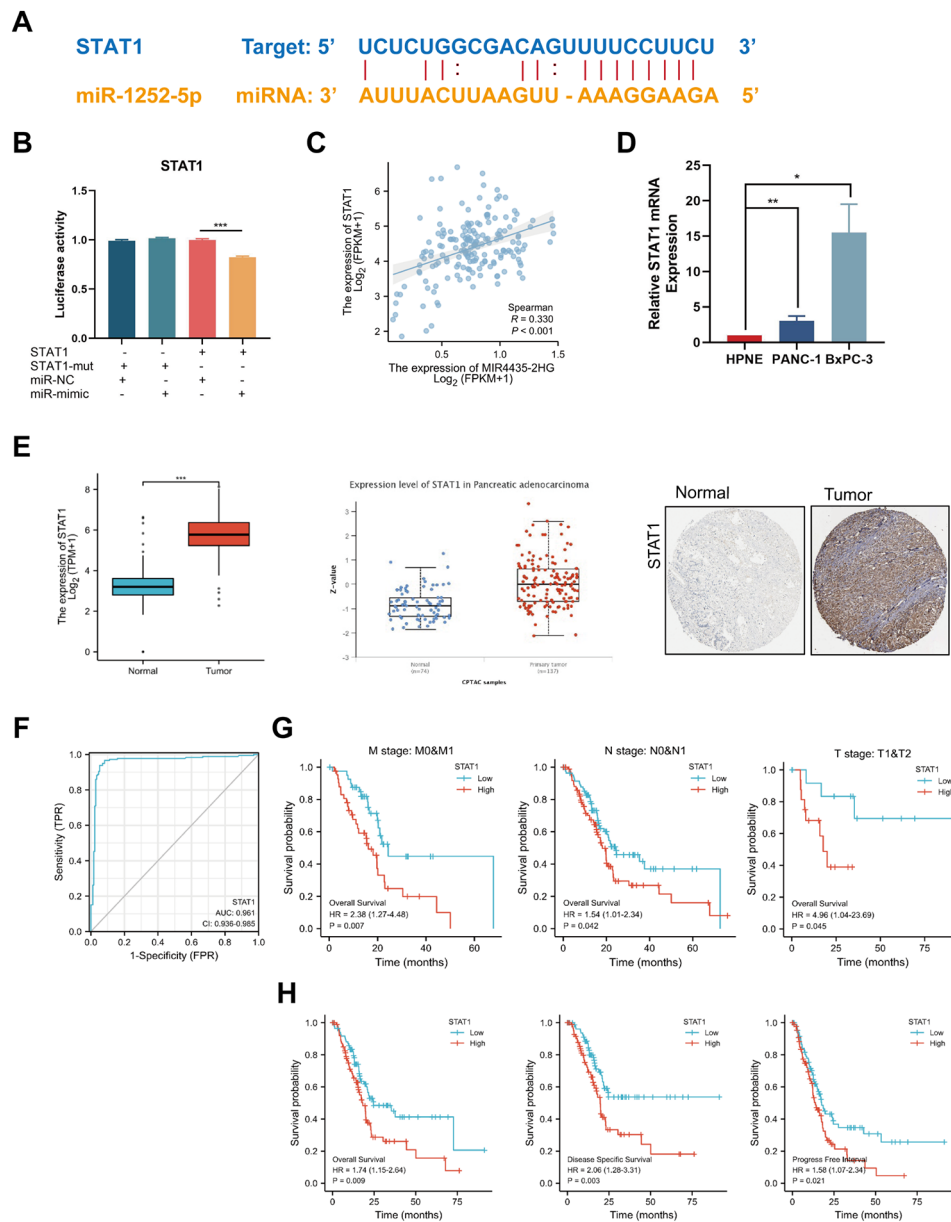


**Fig. 6** STAT1 as a direct target of miR-1252-5p in pancreatic cancer. **(A)** Predicted binding sites for miR-1252-5p on the 3'-UTR of STAT1. **(B)** Dual-luciferase reporter assay showing a significant reduction in luciferase activity in cells transfected with wild-type miR-1252-5p luciferase vectors. **(C)** Positive correlation between STAT1 expression and MIR4435-2HG co-expression. **(D)** RT-qPCR analysis of STAT1 expression in HPNE, BxPC-3, and PANC-1 cells. **(E)** Analysis of STAT1 expression in pancreatic cancer using the TCGA, UALCAN, and Human Protein Atlas databases. **(F)** ROC curve indicating the diagnostic sensitivity and specificity of STAT1 in pancreatic cancer patients. **(G)** Kaplan-Meier survival analysis of STAT1 expression in pancreatic cancer patients based on clinical-pathological features from the TCGA dataset. **(H)** Kaplan-Meier survival analysis comparing overall survival, disease-specific survival, and progression-free interval between STAT1-high and STAT1-low expression groups in pancreatic cancer patients. \* $p < 0.05$ , \*\* $p < 0.01$ , \*\*\* $p < 0.001$

linked to reduced overall survival, disease-specific survival, and progression-free interval, indicating a poor prognosis for patients with pancreatic cancer (Fig. 6H).

#### Enforced STAT1 expression promote PDDA stemness

The mechanism by which STAT1 mediates the effects of the MIR4435-2HG/miR-1252-5p axis remains to be elucidated. To investigate this, we conducted qPCR assays

to analyze STAT1 expression levels. We found that STAT1 was upregulated following the overexpression of MIR4435-2HG or the silencing of miR-1252-5p, while its expression was repressed when MIR4435-2HG was inhibited or miR-1252-5p was overexpressed (Fig. 7A and B).

Additionally, we observed that the overexpression of STAT1 significantly enhanced both sphere formation

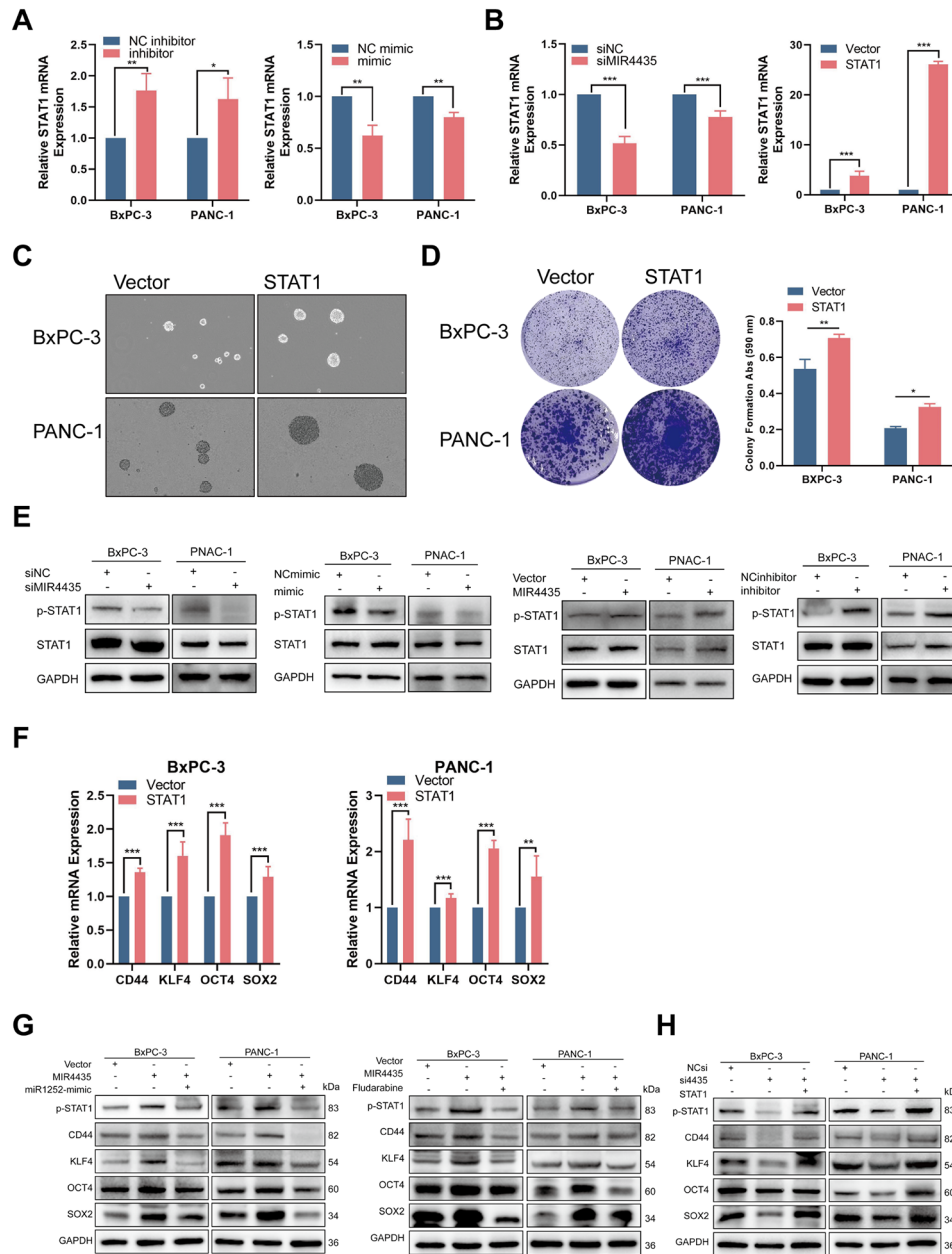


**Fig. 7** Enforced expression of STAT1 promotes pancreatic cancer stemness. **(A)** RT-qPCR analysis of STAT1 expression in cells transfected with miR-1252-5p inhibitor or mimic. **(B)** RT-qPCR analysis of STAT1 expression in cells with MIR4435-2HG knockdown or overexpression. **(C)** Representative images of CSC spheres in cells with STAT1 overexpression. **(D)** Colony formation assay and quantification in BxPC-3 and PANC-1 cells with STAT1 overexpression. **(E)** Western blot analysis of STAT1 and phospho-STAT1 expression in MIR4435-2HG knockdown cells, miR-1252-5p mimic cells, MIR4435-2HG overexpressing cells, and miR-1252-5p inhibitor-transfected cells. **(F)** RT-qPCR analysis of CD44, KLF4, OCT4, and SOX2 expression in cells with STAT1 overexpression. **(G)** Western blot analysis of phospho-STAT1, CD44, KLF4, OCT4, and SOX2 expression in cells co-transfected with MIR4435-2HG and miR-1252-5p mimic, or in MIR4435-2HG-overexpressing cells treated with fludarabine. **(H)** Western blot analysis of phospho-STAT1, CD44, KLF4, OCT4, and SOX2 expression in MIR4435-2HG knockdown cells with enforced STAT1 expression. \* $p < 0.05$ , \*\* $p < 0.01$ , \*\*\* $p < 0.001$

and colony formation abilities in our assays (Fig. 7C and D). Western blot analyses further demonstrated that knockdown MIR4435-2HG or overexpression of miR-1252-5p led to a suppression of STAT1 phosphorylation. Conversely, we detected a significant increase in STAT1 phosphorylation in cells transfected with the

MIR4435-2HG plasmid or treated with a miR-1252-5p inhibitor (Fig. 7E).

In addition, qPCR analysis revealed a marked increase in the expression of stemness markers, such as CD44, KLF4, OCT4, and SOX2, following STAT1 overexpression (Fig. 7F). A similar increase in these markers was observed in cells overexpressing MIR4435-2HG.

However, when co-transfected with miR-1252-5p mimics or treated with the STAT1 inhibitor Fludarabine, we observed a reversal in both STAT1 phosphorylation levels and the expression of CD44, KLF4, OCT4, and SOX2 (Fig. 7G). Moreover, MIR4435-2HG knockdown resulted in decreased STAT1 phosphorylation and reduced expression of stem cell markers. Interestingly, this effect was reversed upon STAT1 overexpression (Fig. 7H). Taken together, these findings indicate that STAT1 is essential in regulating the stemness promoted by the MIR4435-2HG/miR-1252-5p axis in pancreatic ductal adenocarcinoma.

#### **MIR4435-2HG/miR-1252-5p/STAT1 pathway is essential for pancreatic cancer stemness in vivo**

To further investigate the effects of MIR4435-2HG on pancreatic cancer stem cells in vivo, we conducted xenograft experiments using mouse models. We subcutaneously injected  $1 \times 10^6$  BxPC-3 cells, either with MIR4435-2HG knockdown or as a control, into the right flank of athymic nude mice. Consistent with our previous in vitro findings, the knockdown the expression of MIR4435-2HG significantly inhibited pancreatic cancer cell-derived xenografts proliferation, while having no notable impact on the body weight of the mice (Fig. 8A and B).

Further measurements revealed that xenografts derived from BxPC-3 cells with MIR4435-2HG inhibition displayed reduced tumor volumes and lower weights compared to those in the control group (Fig. 8C and D). Flow cytometry analysis indicated that the knockdown of MIR4435-2HG resulted in a significant reduction in the proportion of CD44<sup>+</sup> cells, which are indicative of cancer stem cell populations (Fig. 8E).

Immunohistochemistry assays of the xenografts derived from MIR4435-2HG knockdown pancreatic cancer cells demonstrated a decrease in the expression of the proliferation marker Ki67, suggesting reduced cell proliferation within the tumors. Furthermore, we observed that the MIR4435-2HG/miR-1252-5p/STAT1 axis contributed to the regulating of cancer stem cell properties, as indicated by decreased levels of KLF4, CD44, and phosphorylated STAT1 (p-STAT1) in the xenografts tumors (Fig. 8F). Collectively, our results clearly demonstrate that MIR4435-2HG plays a key role in modulating pancreatic cancer stemness both in vitro and in vivo.

#### **MIR4435-2HG sensitized pancreatic cancer stem cell to ferroptosis**

Due to the dysregulation of iron metabolism in cancer stem cells (CSCs), we investigated whether MIR4435-2HG could sensitize CSC-like cells to ferroptosis. As illustrated in Fig. 9A, key regulators of ferroptosis, SLC7A11 and GPX4, exhibited high involvement, with

their protein expression levels positively correlating with MIR4435-2HG (Fig. 9B). Therefore, we conducted CCK8 assay to elucidate the role of MIR4435-2HG in gemcitabine resistance in pancreatic cancer. The results showed that silencing MIR4435-2HG significantly decreased the IC<sub>50</sub> of gemcitabine, suggesting increased sensitivity. In contrast, overexpression of MIR4435-2HG partially countered this effect, suggesting its involvement in promoting gemcitabine resistance (Fig. 9C). To validate the role of the MIR4435-2HG/miR-1252-5p/STAT1 axis in this resistance mechanism, we upregulated STAT1 in cells with MIR4435-2HG knockdown, which restored cell viability (Fig. 9C). To confirm the regulatory role of the MIR4435-2HG/miR-1252-5p/STAT1 axis in gemcitabine resistance, we upregulated STAT1 expression in cells with MIR4435-2HG knockdown, leading to a reversal in cell viability (Fig. 9D). Moreover, when treated with RSL3, a known ferroptosis inducer, cell viability significantly decreased compared to treatment with gemcitabine alone (Fig. 9E), suggesting that ferroptosis may play a critical role in overcoming gemcitabine resistance.

To investigate this further, we utilized the DHE probe to measure lipid reactive oxygen species (ROS) levels and analyzed the data using flow cytometry. Interestingly, the flow cytometry results demonstrated that STAT1 restored lipid peroxidation levels in MIR4435-2HG knockdown cells (Fig. 9F). Additionally, in gemcitabine-treated cells, knockdown of MIR4435-2HG resulted in decreased release of extracellular ATP, an effect that was reversed by STAT1 transfection. This indicates that STAT1 is involved in modulating the gemcitabine response in relation to MIR4435-2HG expression (Fig. 9G).

Since lipid peroxidation is a key indicator of ferroptosis, we measured lipid peroxidation levels in BxPC-3 and PANC-1 cells with MIR4435-2HG knockdown and STAT1 overexpression. Results showed that MIR4435-2HG knockdown cells had a lower GSH/GSSG ratio, indicating elevated lipid peroxidation (Fig. 9G). Furthermore, given that iron overload is another hallmark of ferroptosis, we measured cytosolic Fe<sup>2+</sup> levels using iron-specific probes. We found that Fe<sup>2+</sup> content was increased in MIR4435-2HG knockdown cells, correlating with heightened radiosensitivity, though this effect was reversed in cells stably overexpressing STAT1.

In summary, these findings suggest that MIR4435-2HG knockdown enhances sensitivity to ferroptosis in pancreatic cancer cells, indicating that modulating ferroptosis could presents a promising therapeutic strategy to overcome chemoresistance in pancreatic cancer (Fig. 10).

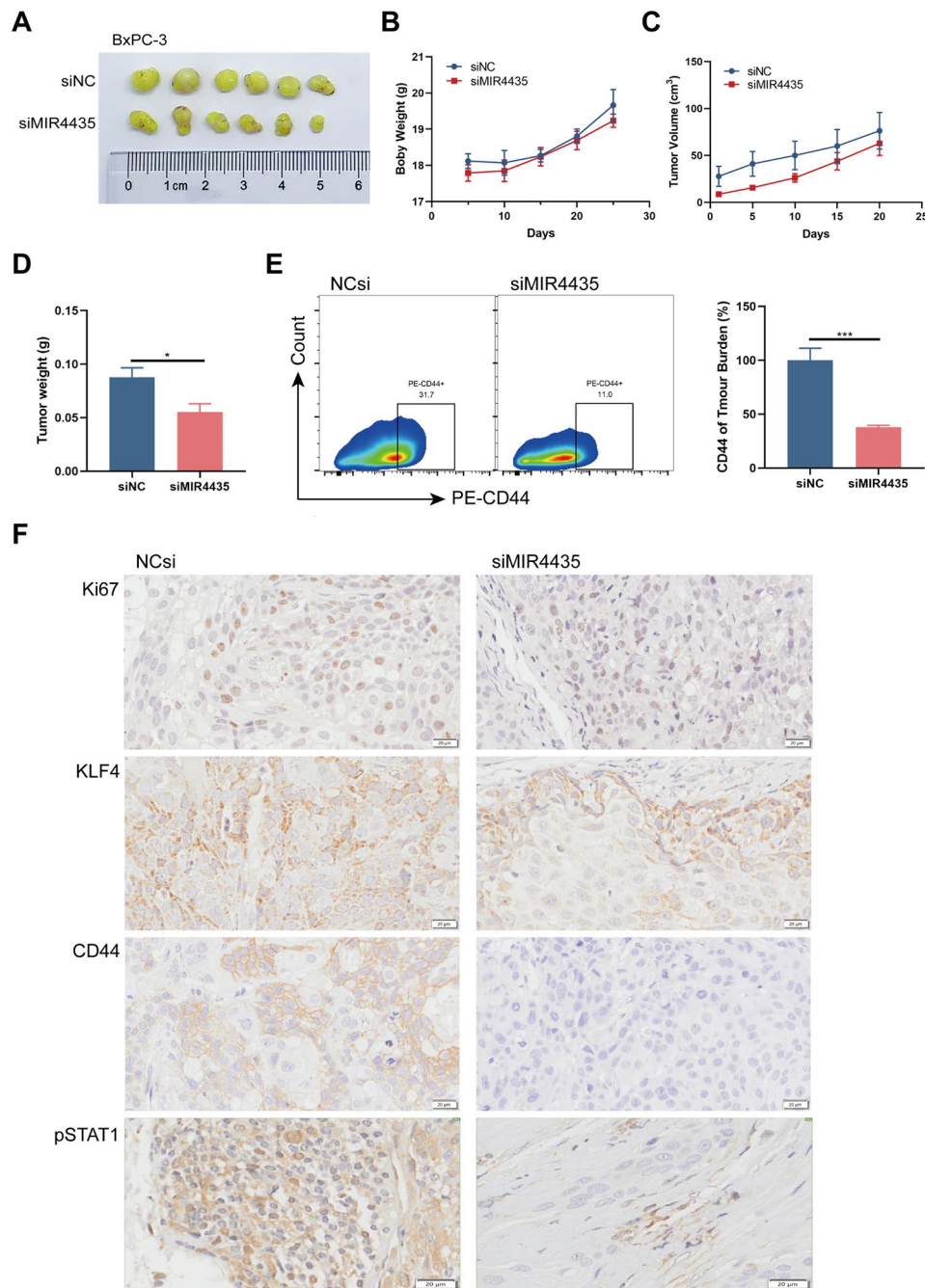


**Fig. 8** The MIR4435-2HG/miR-1252-5p/STAT1 pathway is critical for pancreatic cancer stemness in vivo. **(A)** Representative images of subcutaneous xenografts from BxPC-3 cells with MIR4435-2HG knockdown (n=6). **(B)** Body weight of mice bearing subcutaneous xenografts. **(C)** Tumor volume and **(D)** tumor weight of xenografts. **(E)** Flow cytometry plots showing the percentage of CD44+ cells in MIR4435-2HG knockdown xenograft tumors. **(F)** Representative immunohistochemistry (IHC) images of Ki67, KLF4, CD44, and phosphorylated STAT1 (p-STAT1) in xenograft tumor tissues. \*p<0.05, \*\*p<0.01, \*\*\*p<0.001

## Discussion

Emerging evidence identified the critical role of lncRNAs in controlling cell fate and driving cancer progression, positioning them as key regulators in pancreatic cancer development and potential therapeutic targets [12, 13]. In our study, we identified a marked upregulation

of lncRNA MIR4435-2HG, which functions as an oncogenic driver promoting self-renewal and tumorigenesis in pancreatic cancer. Mechanistic investigations revealed a novel regulatory axis comprising lncRNA MIR4435-2HG, miR-1252-5p, and STAT1 in pancreatic cancer. Importantly, MIR4435-2HG overexpression conferred

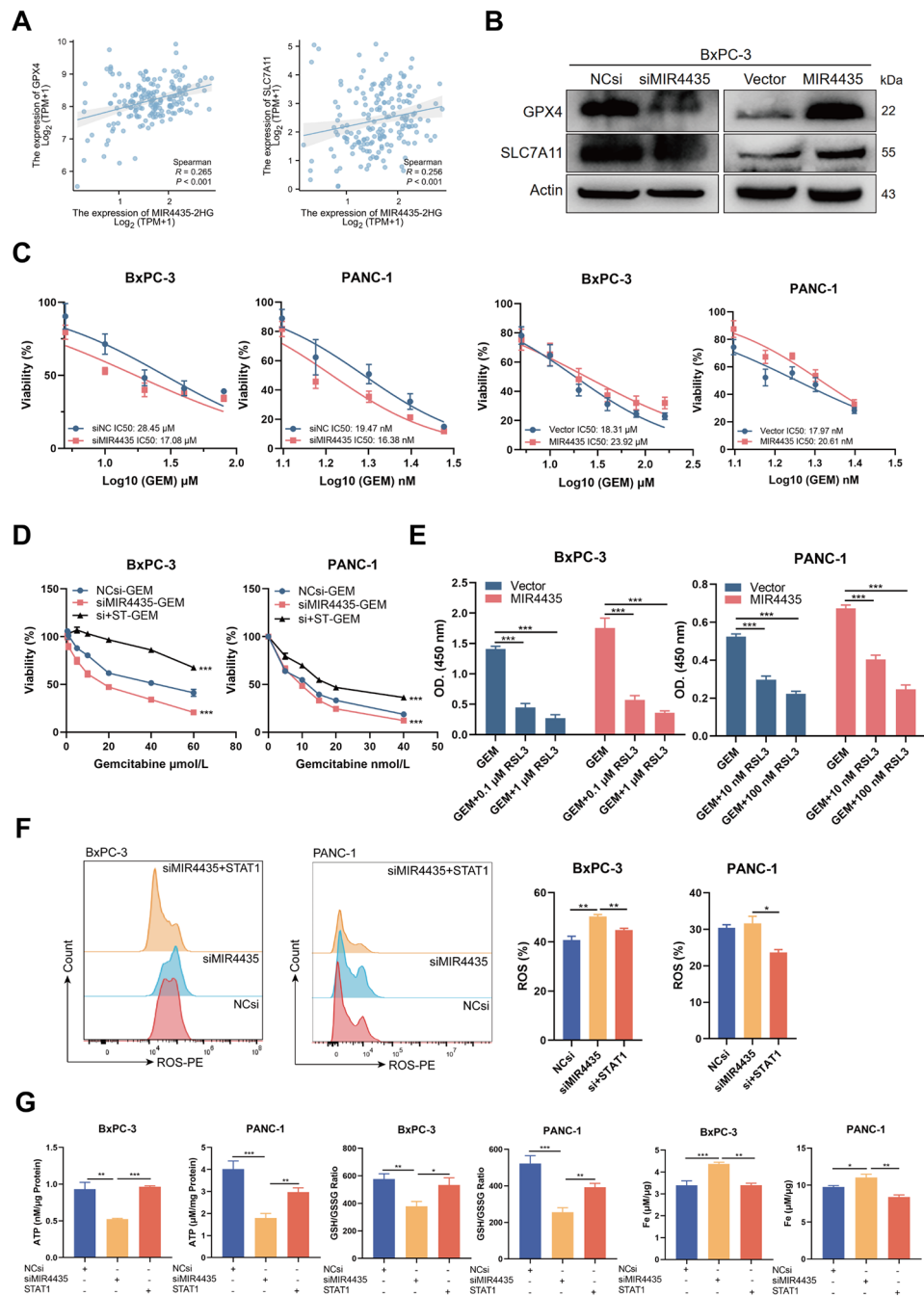


**Fig. 9** MIR4435-2HG sensitizes pancreatic cancer stem cells to ferroptosis. **(A)** The expression levels of GPX4 and SLC7A11 positively correlate with the co-expression of MIR4435-2HG. **(B)** Western blot analysis of GPX4 and SLC7A11 in cells with MIR4435-2HG knockdown and overexpression. **(C)** Relative cell viability and IC50 values for MIR4435-2HG knockdown and overexpressing cells following gemcitabine (GEM) treatment. **(D)** Relative cell viability of MIR4435-2HG knockdown cells co-transfected with STAT1 after gemcitabine (GEM) therapy. **(E)** Relative OD450 values for BxPC-3 control and MIR4435-2HG overexpressing cells treated with GEM, GEM + 0.1 μM RSL3, and GEM + 1 μM RSL3. Corresponding OD450 values for PANC-1 control and MIR4435-2HG overexpressing cells treated with GEM, GEM + 10 nM RSL3, and GEM + 100 nM RSL3. **(F)** Representative flow cytometry plots showing ROS levels and percentages in MIR4435-2HG knockdown cells and those co-transfected with STAT1. **(G)** Measurement of ATP levels, GSH levels, and iron content in MIR4435-2HG knockdown cells and MIR4435-2HG co-transfected with STAT1 cells \*p<0.05, \*\*p<0.01, \*\*\*p<0.001

resistance to gemcitabine, which induced cell death partly through ferroptosis.

Recent research has emphasized the critical role of MIR4435-2HG in a range of biological processes.

demonstrating its oncogenic functions across multiple cancer types [14]. It has been consistently found to be upregulated in hepatocellular carcinoma [15, 16], gastric cancer [17], esophageal squamous cell carcinoma [18],

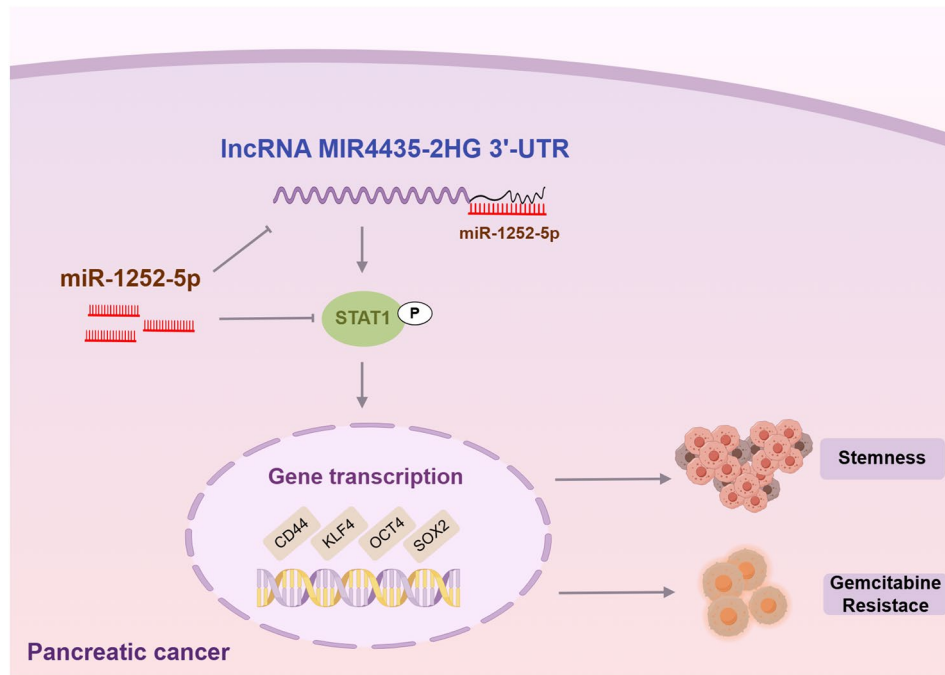


**Fig. 10** A proposed model illustrating how MIR4435-2HG targets the miR-1252-5p/STAT1 axis to regulate pancreatic cancer stem cell and gemcitabine sensitivity

colorectal cancer [19] and pancreatic cancer, where its overexpression associated with advanced tumor stages, larger tumor sizes, lymph node metastasis, and poor overall survival [20]. Knock down MIR4435-2HG significantly inhibited the progression of pancreatic cancer by miR-128-3p/ABHD17C. Functionally, MIR4435-2HG promotes cancer cell proliferation by influencing cell cycle regulation and altering metabolic pathways, including glucose and glutamine metabolism. It interacts with key cell cycle regulators, such as BRCA2 and CCND1, and plays a crucial role in remodeling glutamine metabolism to meet the biosynthetic demands of rapidly proliferating cancer cells [21]. The oncogenic effects of MIR4435-2HG are partially mediated through epigenetic modifications and its involvement in critical signaling pathways, including TGF- $\beta$  [22], Wnt/ $\beta$ -catenin, and mTOR [23], which promote cancer cell migration, invasion, and maintenance of stemness, contributing to drug resistance. In the present study, we found that MIR4435-2HG sustain stemness and promote chemoresistance, which were in consistency with the researches.

To investigate the potential mechanism by which MIR4435-2HG contributes to the development of pancreatic adenocarcinoma, our functional assays revealed that MIR4435-2HG acts as an upstream regulator of miR-1252-5p. Additionally, the luciferase reporter assay confirmed that miR-1252-5p directly interacts with MIR4435-2HG. Notably, miR-1252-5p is known to function as an antitumor miRNA in various human cancers,

including non-small cell lung cancer and papillary thyroid cancer [24], and is associated with ovarian cancer drug resistance. Notably, miR-1252-5p is significantly downregulated in pancreatic cancer tissues and cell lines, where it plays a critical role in inhibiting the proliferation, migration, invasion, and epithelial-mesenchymal transition of pancreatic cells [25]. In line with these findings, our current study demonstrated through gain- and loss-of-function experiments that overexpression of miR-1252-5p effectively inhibited cell stemness and proliferation, while its knockdown promoted aggressive behaviors. Furthermore, analyses using TargetScan and StarBase databases identified STAT1 as a direct target gene of miR-1252-5p. Public databases have also confirmed a positive correlation between MIR4435-2HG and STAT1 expression. Additionally, previous research has shown that STAT1 typically functions as a transcription factor within the tumor immune response via the NF- $\kappa$ B signaling pathway, playing a key role in mediating cancer progression and tumorigenesis [26, 27]. In addition, the oncogenic role of STAT1 on pancreatic cancer has been studied as well. PD-L1 was transcriptionally regulated by STAT1 and lncRNA PSMB8-AS1 in PC cells [28]. In fumarate hydratase (FH)-deficient renal cell carcinoma (RCC), the accumulation of fumarate leads to the upregulation of MIR4435-2HG expression through H3K4me3 histone modification, which is mediated by the activation of the STAT1/GLS1 signaling pathway [29].

MIR4435-2HG has been implicated in drug resistance across multiple cancer types, including resistance to resveratrol in lung cancer [30], cisplatin in non-small cell lung cancer and colorectal cancer [31, 32], and carboplatin in triple-negative breast cancer [33]. In pancreatic cancer, gemcitabine combined with nab-paclitaxel remains the standard first-line chemotherapy regimen, underscoring the critical role of gemcitabine in treating advanced and metastatic disease [34]. However, despite its clinical efficacy, chemoresistance to gemcitabine is a significant challenge, compromising its therapeutic potential and contributing to poor outcomes [35]. Recent studies have highlighted that enhancing ferroptosis could offer a promising strategy to improve the clinical effectiveness of chemotherapy, including pancreatic cancer [36]. Mechanistically, gemcitabine induces the generation of reactive oxygen species (ROS), which contributes to its cytotoxic effects. However, this accumulation of ROS can paradoxically activate antioxidant defense mechanisms, thereby promoting chemoresistance [37]. Specifically, ROS activates NRF2, a key regulator of the cellular antioxidant response, which drives the expression of genes involved in glutathione (GSH) synthesis [38]. The NRF2/KEAP1 axis, therefore, plays a pivotal role in regulating both ferroptosis sensitivity and gemcitabine resistance, making it an important therapeutic target. In parallel, recent studies have elucidated the role of the glutamine transporter SLC38A5 in gemcitabine resistance in pancreatic cancer. Specifically, SLC38A5 is overexpressed in gemcitabine-resistant pancreatic ductal adenocarcinoma (PDAC) cells, and its inhibition sensitizes these cells to gemcitabine by triggering ferroptosis [39]. Inhibition of SLC38A5 results in decreased glutamine uptake, reduced GSH levels, and the downregulation of GSH-related genes, including NRF2 and GPX4. This mechanism aligns with the findings in our study, where MIR4435-2HG regulates ferroptosis through modulate antioxidant defenses and lipid metabolism. Additionally, studies investigating ferroptosis-related long non-coding RNAs (lncRNAs) in colon cancer and papillary renal cell carcinoma have suggested that MIR4435-2HG may act as a biomarker linked to immune infiltration, tumor progression, and chemoresistance [40, 41]. These findings further support the hypothesis that MIR4435-2HG could play a crucial role in modulating ferroptosis, enhancing chemoresistance, and contributing to tumor progression. Targeting MIR4435-2HG may, therefore, represent a novel therapeutic strategy to modulate ferroptosis and potentially overcome chemoresistance in pancreatic cancer.

## Conclusion

In conclusion, this study emphasizes the oncogenic role of MIR4435-2HG in promoting cancer stem cell properties, tumor progression, and chemoresistance in

pancreatic cancer via the miR-1252-5p/STAT1 axis. Furthermore, the MIR4435-2HG-mediated inhibition of ferroptosis presents a potential therapeutic target to address chemoresistance in pancreatic cancer.

## Supplementary Information

The online version contains supplementary material available at <https://doi.org/10.1186/s12967-025-06128-8>.

Supplementary Material 1

Supplementary Material 2

Supplementary Material 3

Supplementary Material 4

## Author contributions

LXH designed the study and conceived the project. BCX and PSW collected the data from several databases, HYL and XDY reviewed the results and revised the manuscript. All authors reviewed manuscript.

## Funding

This work was supported by funds from the Guangdong Basic and Applied Basic Research Foundation, China (No. 2021B1515140031 and 2020A1515110029), Dongguan Science and Technology of Social Development Program, China (No. 2019507163147 and 20211800905042). The Tenth Affiliated Hospital of Southern Medical University (Dongguan People's Hospital) Dongguan People's Hospital (No. K202009 and Z202412).

## Data availability

The datasets supporting the conclusions of this article are available in the TCGA and GEO cohorts.

## Declarations

### Ethics approval and consent to participate

All patients have signed an informed consent form, and the study protocol has acquired official approval from The Tenth Affiliated Hospital of Southern Medical University.

### Consent for publication

Not applicable.

### Competing interests

The authors declare that they have no competing interests.

Received: 27 November 2024 / Accepted: 9 January 2025

Published online: 07 February 2025

## References

1. Dreyer SB, Rae S, Bisset K, Upstill-Goddard R, Gemenetzis G, Johns AL, Dickson EJ, Mittal A, Gill AJ, Duthie F, Pea A, Lawlor RT, Scarpa A, Salvia R, Pulvirenti A, Zerbi A, Marchesi F, McKay CJ, Biankin AV, Samra JS, Chang DK, Jamieson NB. The impact of Molecular Subtyping on pathological staging of pancreatic Cancer. *ANN SURG*. 2023;277:e396–405.
2. Hermann PC, Huber SL, Herrler T, Aicher A, Ellwart JW, Guba M, Bruns CJ, Heeschen C. Distinct populations of cancer stem cells determine tumor growth and metastatic activity in human pancreatic cancer. *Cell Stem Cell*. 2007;1:313–23.
3. Ishiwata T, Matsuda Y, Yoshimura H, Sasaki N, Ishiwata S, Ishikawa N, Takubo K, Arai T, Aida J. Pancreatic cancer stem cells: features and detection methods. *PATHOL ONCOL RES*. 2018;24:797–805.
4. Yang Y, Wen L, Zhu H. Unveiling the hidden function of long non-coding RNA by identifying its major partner-protein. *CELL BIOSCI*. 2015;5:59.
5. Gutschner T, Diederichs S. The hallmarks of cancer: a long non-coding RNA point of view. *RNA BIOL*. 2012;9:703–19.

6. Loewer S, Cabili MN, Guttman M, Loh YH, Thomas K, Park IH, Garber M, Curran M, Onder T, Agarwal S, Manos PD, Datta S, Lander ES, Schlaeger TM, Daley GQ, Rinn JL. Large intergenic non-coding RNA-RoR modulates reprogramming of human induced pluripotent stem cells. *NAT GENET.* 2010;42:1113–17.
7. Wang Y, Xu Z, Jiang J, Xu C, Kang J, Xiao L, Wu M, Xiong J, Guo X, Liu H. Endogenous miRNA sponge lincRNA-RoR regulates Oct4, nanog, and Sox2 in human embryonic stem cell self-renewal. *DEV CELL.* 2013;25:69–80.
8. Shen H, Sun B, Yang Y, Cai X, Bi L, Deng L, Zhang L. MIR4435-2HG regulates cancer cell behaviors in oral squamous cell carcinoma cell growth by upregulating TGF-beta1. *ODONTOLOGY.* 2020;108:553–59.
9. Zhang S, Li C, Liu J, Geng F, Shi X, Li Q, Lu Z, Pan Y. Fusobacterium nucleatum promotes epithelial-mesenchymal transition through regulation of the lincRNA MIR4435-2HG/miR-296-5p/Akt2/SNA1 signaling pathway. *FEBS J.* 2020;287:4032–47.
10. Zhang M, Yu X, Zhang Q, Sun Z, He Y, Guo W. MIR4435-2HG: a newly proposed lincRNA in human cancer. *BIOMED PHARMACOTHER.* 2022;150:112971.
11. Zhong C, Xie Z, Zeng LH, Yuan C, Duan S. MIR4435-2HG is a potential Pan-cancer Biomarker for diagnosis and prognosis. *FRONT IMMUNOL.* 2022;13:855078.
12. McCabe EM, Rasmussen TP. lncRNA involvement in cancer stem cell function and epithelial-mesenchymal transitions. *SEMIN CANCER BIOL.* 2021;75:38–48.
13. Zhou L, Zhu Y, Sun D, Zhang Q. Emerging roles of long non-coding RNAs in the Tumor Microenvironment. *INT J BIOL SCI.* 2020;16:2094–103.
14. Ke D, Li H, Zhang Y, An Y, Fu H, Fang X, Zheng X. The combination of circulating long noncoding RNAs AK001058, lincRNA-AS1, MIR4435-2HG, and CEBPA-AS1 fragments in plasma serve as diagnostic markers for gastric cancer. *Oncotarget.* 2017;8:21516–25.
15. Xu X, Gu J, Ding X, Ge G, Zang X, Ji R, Shao M, Mao Z, Zhang Y, Zhang J, Mao F, Qian H, Xu W, Cai H, Wang F, Zhang X. LINC00978 promotes the progression of hepatocellular carcinoma by regulating EZH2-mediated silencing of p21 and E-cadherin expression. *CELL DEATH DIS.* 2019;10:752.
16. Shen X, Ding Y, Lu F, Yuan H, Luan W. Long noncoding RNA MIR4435-2HG promotes hepatocellular carcinoma proliferation and metastasis through the miR-22-3p/YWHAZ axis. *AM J TRANSL RES.* 2020;12:6381–94.
17. Wang H, Wu M, Lu Y, He K, Cai X, Yu X, Lu J, Teng L. lncRNA MIR4435-2HG targets desmoplakin and promotes growth and metastasis of gastric cancer by activating Wnt/beta-catenin signaling. *Aging.* 2019;11:6657–73.
18. Zong MZ, Shao Q, An XS. Expression and prognostic significance of long noncoding RNA AK001796 in esophageal squamous cell carcinoma. *EUR REV MED PHARMACO.* 2019;23:181–86.
19. Bai J, Xu J, Zhao J, Zhang R. Downregulation of lincRNA AWWPPH inhibits colon cancer cell proliferation by downregulating GLUT-1. *ONCOL LETT.* 2019;18:2007–12.
20. Chen Z, Du Y, Shi H, Dong S, He R, Zhou W. Long non-coding RNA MIR4435-2HG promotes pancreatic cancer progression by regulating ABHD17C through sponging miR-128-3p. *TRANSL CANCER RES.* 2024;13:4113–30.
21. Pei L, Yan D, He Q, Kong J, Yang M, Ruan H, Lin Q, Huang L, Huang J, Lin T, Qin H. lncRNA MIR4435-2HG drives cancer progression by modulating cell cycle regulators and mTOR signaling in stroma-enriched subtypes of urothelial carcinoma of the bladder. *CELL ONCOL.* 2023;46:1509–27.
22. Zhang H, Meng H, Huang X, Tong W, Liang X, Li J, Zhang C, Chen M. lncRNA MIR4435-2HG promotes cancer cell migration and invasion in prostate carcinoma by upregulating TGF-beta1. *ONCOL LETT.* 2019;18:4016–21.
23. Hartana CA, Rassadkina Y, Gao C, Martin-Gayo E, Walker BD, Lichtenfeld M, Yu XG. Long noncoding RNA MIR4435-2HG enhances metabolic function of myeloid dendritic cells from HIV-1 elite controllers. *J CLIN INVEST.* 2021;131.
24. Tian X, Zhang L, Jiao Y, Chen J, Shan Y, Yang W. CircABC10 promotes nonsmall cell lung cancer cell proliferation and migration by regulating the miR-1252/FOXR2 axis. *J CELL BIOCHEM.* 2019;120:3765–72.
25. Xue Y, Wu T, Sheng Y, Zhong Y, Hu B, Bao C. MicroRNA-1252-5p, regulated by myb, inhibits invasion and epithelial-mesenchymal transition of pancreatic cancer cells by targeting NEDD9. *Aging.* 2021;13:18924–45.
26. Yang L, Dong Y, Li Y, Wang D, Liu S, Wang D, Gao Q, Ji S, Chen X, Lei Q, Jiang W, Wang L, Zhang B, Yu JJ, Zhang Y. IL-10 derived from M2 macrophage promotes cancer stemness via JAK1/STAT1/NF-kappaB/Notch1 pathway in non-small cell lung cancer. *INT J CANCER.* 2019;145:1099–110.
27. Eilion DL, Jacobson ME, Hicks DJ, Rahman B, Sanchez V, Gonzales-Ericson PI, Fedorova O, Pyle AM, Wilson JT, Cook RS. Therapeutically active RIG-I agonist induces immunogenic Tumor Cell killing in breast cancers. *CANCER RES.* 2018;78:6183–95.
28. Zhang H, Zhu C, He Z, Chen S, Li L, Sun C. lncRNA PSM8-AS1 contributes to pancreatic cancer progression via modulating miR-382-3p/STAT1/PD-L1 axis. *J EXP CLIN CANC RES.* 2020;39:179.
29. Zhang Y, Liu Z, Yang X, Lu W, Chen Y, Lin Y, Wang J, Lin S, Yun JP. H3K27 acetylation activated-COL6A1 promotes osteosarcoma lung metastasis by repressing STAT1 and activating pulmonary cancer-associated fibroblasts. *THERANOSTICS.* 2021;11:1473–92.
30. Yang Q, Xu E, Dai J, Liu B, Han Z, Wu J, Zhang S, Peng B, Zhang Y, Jiang Y. A novel long noncoding RNA AK001796 acts as an oncogene and is involved in cell growth inhibition by resveratrol in lung cancer. *TOXICOL APPL PHARM.* 2015;285:79–88.
31. Liu B, Pan CF, Ma T, Wang J, Yao GL, Wei K, Chen YJ. Long non-coding RNA AK001796 contributes to cisplatin resistance of non-small cell lung cancer. *MOL MED REP.* 2017;16:4107–12.
32. Luo P, Wu S, Ji K, Yuan X, Li H, Chen J, Tian Y, Qiu Y, Zhong X. lncRNA MIR4435-2HG mediates cisplatin resistance in HCT116 cells by regulating Nrf2 and HO-1. *PLoS ONE.* 2020;15:e223035.
33. Liu AN, Qu HJ, Gong WJ, Xiang JY, Yang MM, Zhang W. lncRNA AWWPPH and miRNA-21 regulates cancer cell proliferation and chemosensitivity in triple-negative breast cancer by interacting with each other. *J CELL BIOCHEM.* 2019;120:14860–66.
34. Meneses-Medina MI, Gervaso L, Cella CA, Pellicori S, Gandini S, Sousa MJ, Fazio N. Chemotherapy in pancreatic ductal adenocarcinoma: when cyto-reduction is the aim. A systematic review and meta-analysis. *CANCER TREAT REV.* 2022;104:102338.
35. Liang C, Shi S, Meng Q, Liang D, Ji S, Zhang B, Qin Y, Xu J, Ni Q, Yu X. Complex roles of the stroma in the intrinsic resistance to gemcitabine in pancreatic cancer: where we are and where we are going. *EXP MOL MED.* 2017;49:e406.
36. Friedmann AJ, Krysko DV, Conrad M. Ferroptosis at the crossroads of cancer-acquired drug resistance and immune evasion. *NAT REV CANCER.* 2019;19:405–14.
37. Arlt A, Schafer H, Kalthoff H. The 'N-factors' in pancreatic cancer: functional relevance of NF-kappaB, NFAT and Nrf2 in pancreatic cancer. *ONCOGENESIS.* 2012;1:e35.
38. Zhou Y, Zhou Y, Yang M, Wang K, Liu Y, Zhang M, Yang Y, Jin C, Wang R, Hu R. Digoxin sensitizes gemcitabine-resistant pancreatic cancer cells to gemcitabine via inhibiting Nrf2 signaling pathway. *REDOX BIOL.* 2019;22:101131.
39. Kim MJ, Kim HS, Kang HW, Lee DE, Hong WC, Kim JH, Kim M, Cheong JH, Kim HJ, Park JS. SLC38A5 modulates ferroptosis to overcome Gemcitabine Resistance in Pancreatic Cancer. *CELLS-BASEL.* 2023;12.
40. Dang R, Jin M, Nan J, Jiang X, He Z, Su F, Li D. A Novel ferroptosis-related lncRNA signature for prognosis prediction in patients with Papillary Renal Cell Carcinoma. *INT J GEN MED.* 2022;15:207–22.
41. Chen W, Chen Y, Liu L, Wu Y, Fu P, Cao Y, Xiong J, Tu Y, Li Z, Liu Y, Jie Z. Comprehensive Analysis of Immune infiltrates of ferroptosis-related long noncoding RNA and prediction of Colon cancer patient prognoses. *J IMMUNOL RES.* 2022;2022:9480628.

## Publisher's note

Springer Nature remains neutral with regard to jurisdictional claims in published maps and institutional affiliations.